

Three-axis capacitive force sensor with liquid metal electrodes for endoscopic palpation

Tatsuho Nagatomo , Norihisa Miki

Department of Mechanical Engineering, Keio University, Yokohama 223-8522, Japan
✉ E-mail: tatsuho19950307@keio.jp

Published in *Micro & Nano Letters*; Received on 3rd March 2017; Revised on 24th April 2017; Accepted on 9th May 2017

Endoscopic palpation is a promising technology for detecting tumours that are too small to be detected by CT and magnetic resonance imaging, are not located on tissue surfaces, and cannot be observed using endoscopes. This method uses a small force sensor mounted on the tip of an endoscope. It is desirable that the sensor can scan tissue surfaces and continuously measure the stiffness of organs. Prior work developed a ballpoint-pen-like capacitive force sensor and carried out proof of principle experiments; however, the sensor was too large to be mounted on an endoscope. This study designed three-dimensional (3D) microfluidic channels encapsulating liquid metal to develop a sensor that is small enough to be mounted on an endoscope. Eight polydimethyl siloxane layers with channel structures were assembled and filled with Galinstan, a commercial liquid metal, to form 3D electrodes. The sensor was experimentally characterised and verified to be applicable to endoscopic palpation.

1. Introduction: Endoscopy and magnetic resonance imaging have recently become the two primary methods for cancer screening; however, neither can be used to detect deeply located small tumours [1–3]. Given the higher stiffness of tumour cells than normal cells [4–6], endoscopic palpation using a miniature force sensor mounted to the tip of the endoscope is a promising technology to detect such tumours, which can lead to early detection of cancer.

In our previous work, we proposed a ballpoint-pen-like capacitive sensor that can scan and measure the stiffness of tissues, as illustrated in Fig. 1 [7]. To measure the reaction force, the sensor was equipped with three-dimensional (3D) liquid metal electrodes. Given the cylindrical shape of the sensor, the electrodes forming the capacitors for the three coordinate axes need to be formed in a 3D configuration. Since it is difficult to form such electrodes by patterning metal films using conventional microfabrication techniques, liquid metal was encapsulated in the pockets of a polydimethyl siloxane (PDMS) structure to form the electrodes. However, it was 10 mm in diameter and much too large to be mounted on an endoscope since these pocket-type electrodes were difficult to miniaturise because they became increasingly harder to fill with the highly viscous liquid metal as their size was reduced. Thus, in this study, we miniaturised the electrodes by encapsulating the liquid metal into microchannels formed by stacking soft-lithographically patterned structures, as shown in Fig. 2. We successfully developed the fabrication processes for the sensor. PDMS layers are replicated from the micro-machined PMMA mould and sequentially bonded with liquid PDMS. Galinstan, a commercial liquid metal, is then introduced into the channels and encapsulated with another PDMS thin layer. A three-axis cylindrical capacitive force sensor is completed by adding a rod in the centre, which receives the external forces. The cylindrical shape is beneficial for mounting on an endoscope. The four semi-cylindrical electrodes, with the inner electrodes rotated by 90° with respect to the outer electrodes, form four capacitors that can detect the magnitude and orientation of an applied shear force. The applied force in the normal direction (hereafter, normal force) is measured with another set of electrodes that form a capacitor. We experimentally characterised the device and verified that it can be used as a force sensor for endoscopic palpation.

2. Principle: The force sensor developed in this study measures the force applied to the rod that is positioned in the centre of

the sensor, as shown in Fig. 3. The four capacitors (A–D) formed by four semi-cylindrical electrodes detect the shear force and an additional capacitor detects the normal force. We denote these two sets of sensors as the top and bottom sensors, respectively. Six electrodes are formed in a 3D configuration by microfluidic channels encapsulating liquid metal.

As shown in Fig. 3, the outer and inner electrodes of the top sensor are arranged to surround the rod. A reaction force exerted on the centre rod deforms the sensor, causing a change in capacitance that can be used to determine the magnitude and orientation of the force. Assuming that only the inner electrodes are displaced, the capacitance C of one of the four capacitors can be expressed as follows using Gauss' law:

$$C = \frac{Q}{V} = \frac{\pi\epsilon L}{2 \log |R/x|} \quad (1)$$

where Q and ϵ are the surface charge and dielectric constant of the inner electrode, respectively, x and R are the respective radii of the inner and outer electrodes, and L is the thickness of the PDMS wall. Equation (1) indicates that the capacitance C increases monotonically with x . Therefore, the applied shear force can be deduced from the variation in C .

Using the forces deduced using the four capacitors, the direction of the applied shear force can be obtained. As shown in Fig. 3, F can be decomposed into perpendicular components F_α and F_β , pointing in the direction of two of the four capacitors. Each component can be expressed in terms of the magnitude of F and the angle θ as follows

$$F_\alpha = F \cos(\theta - \delta) \quad (2)$$

$$F_\beta = F \sin(\theta - \delta) \quad (3)$$

where δ depends on the position of the two capacitors of interest, and θ is the angle between F and the y -axis.

The bottom sensor consists of two electrodes facing each other to produce a capacitance, whose variation can be used to determine the normal force. The relationship between the change in capacitance ΔC and the contact force F is given by

$$\Delta C = \alpha_1 F + \frac{\alpha_2}{S} F^2 \quad (4)$$

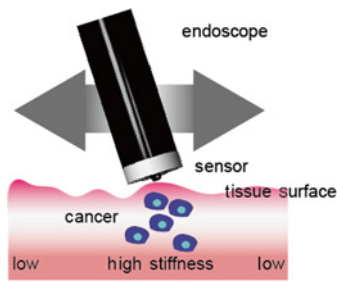


Fig. 1 Concept of endoscopic tissue palpation

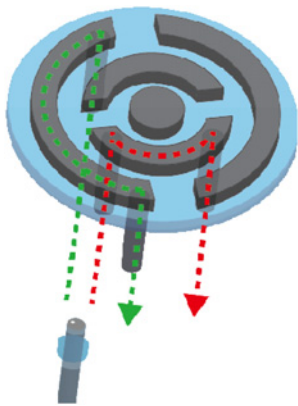


Fig. 2 Microfluidic channels filled with liquid metal to form 3D electrodes

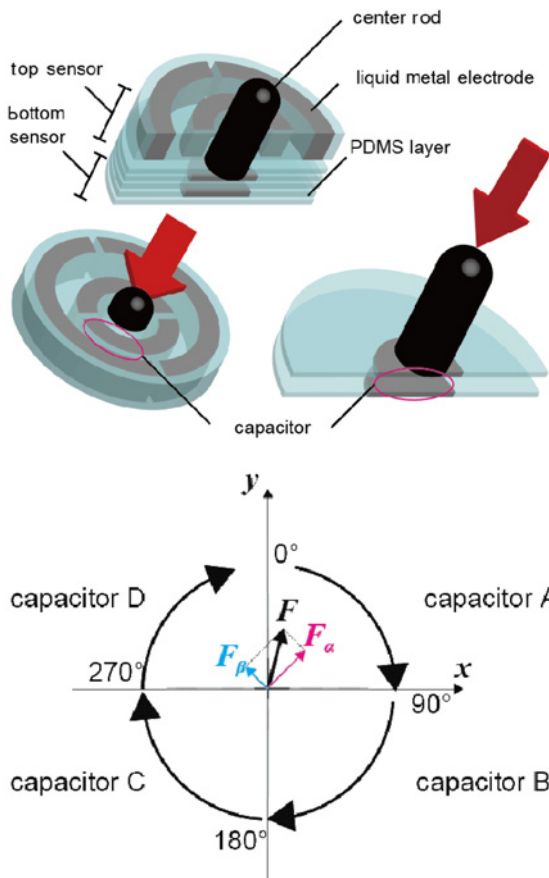


Fig. 3 Concept of 3D force sensor

$$\alpha_m \equiv \frac{\varepsilon(d - d_0)^m}{d^{(m+1)}E^m} \quad (5)$$

where ε is the dielectric constant of the dielectric, d is the equilibrium thickness of the dielectric, d_0 is the resulting thickness of the dielectric when it is compressed to the limit, S is contact area, and $m = 1, 2$ [8].

3. Fabrication process: The fabrication process for the sensor, which is composed of eight PDMS layers, is illustrated in Fig. 4. PDMS is poured into a PMMA mould and cured at 65°C for 6 h. The moulds are machined using a MiniMiller MM-100 (Modia Systems Co., Ltd.), and the PDMS layers are peeled off from the moulds. The liquid PDMS (PDMS:toluene is 2:3 by weight) [9, 11] is spin-coated on a glass plate in advance. The bonding interface of each PDMS layer is placed in contact with the liquid PDMS, and the liquid PDMS is transferred to the bonding surface. The eight layers are stacked and cured at 65°C for 2 h to complete the bonding. We used Galinstan (Liquid PRO, Coollaboratory), which is composed of 68.5% gallium, 21.5% indium, and 10% tin, as the liquid metal. The Galinstan was introduced into the channels using a custom syringe, and excess metal was wiped away using a Kimwipe soaked with ethanol. The miniaturised sensor was successfully fabricated, as shown in Fig. 5. The dimensions of the sensor electrodes are listed in Table 1. The centre rod, which is made of tungsten carbide and is 2.2 mm in diameter and 2.5 mm in length (As ONE Corporation), is manually attached to the top of the sensor.

4. Experimental method: First, the relationship between the magnitude of a shear force applied to the top sensor and the resulting change in capacitance of capacitors A–D was

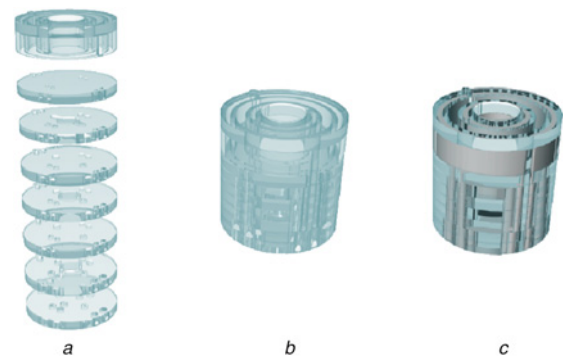


Fig. 4 Fabrication process for sensor.

a Eight layers made of PDMS are replica moulded using PMMA moulds machined with a milling machine [MiniMiller MM-100 (Modia Systems Co., Ltd.)]

b Layers are stacked and glued with liquid PDMS

c Galinstan is introduced into the channels to form 3D microfluidic channels

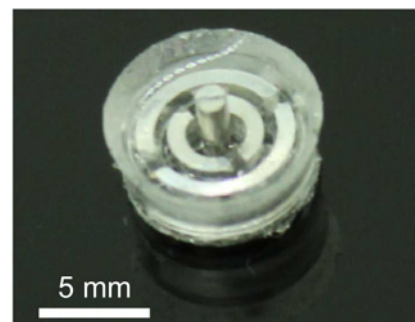


Fig. 5 Photograph of fabricated sensor

Table 1 Dimensions of the sensor electrodes

	Height, mm	Width, mm	Radius, mm	Gap, mm
bottom sensor electrodes	0.25	—	1.20	0.50
inner electrodes	1.00	0.20	1.40	0.40
outer electrodes	1.00	0.20	2.00	0.40

investigated using the experimental system shown in Fig. 6a. The sensor was fixed to a rotation stage, and a compression testing machine (Micro Autograph MST-I, Shimadzu) was used to apply the shear force to the centre rod. The applied force was increased from 0.1 to 1.0 N while measuring the capacitance with an LCR meter. This measurement was carried out four times, at $\theta=45^\circ$, 135° , 225° , and 315° . The measurement frequency was 5.5 MHz and the electromotive force was 1.0 V.

Next, the relationship between the orientation of a shear force applied to the top sensor and the resulting change in capacitance of capacitors A–D (see Fig. 3) was investigated. The force was fixed at 1.0 N, and θ was incremented from 0 to 360° in steps of 15° while monitoring the capacitance.

Finally, the bottom sensor was characterised with respect to the normal force using the experimental setup shown in Fig. 6b. The force was varied from 0.1 to 1.0 N while measuring the capacitance of the bottom sensor with an LCR meter. The measurement frequency was 5.5 MHz and the electromotive force was 1.0 V.

5. Results and discussion: Fig. 7 shows plots of change in capacitance for capacitors A–D when force is applied perpendicular to each capacitor, $\Delta C/C_0$, versus the applied shear

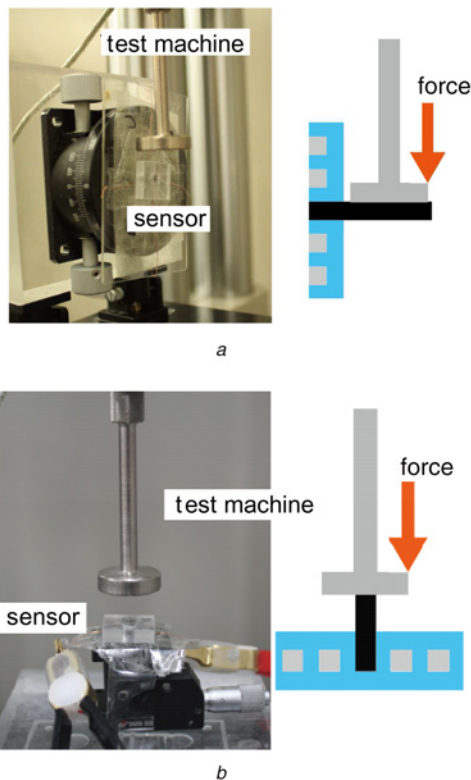


Fig. 6 Experimental setup for
 a Top sensor and
 b Bottom sensor. The top sensor measures the shear force applied to the centre rod and the bottom sensor detects the normal force

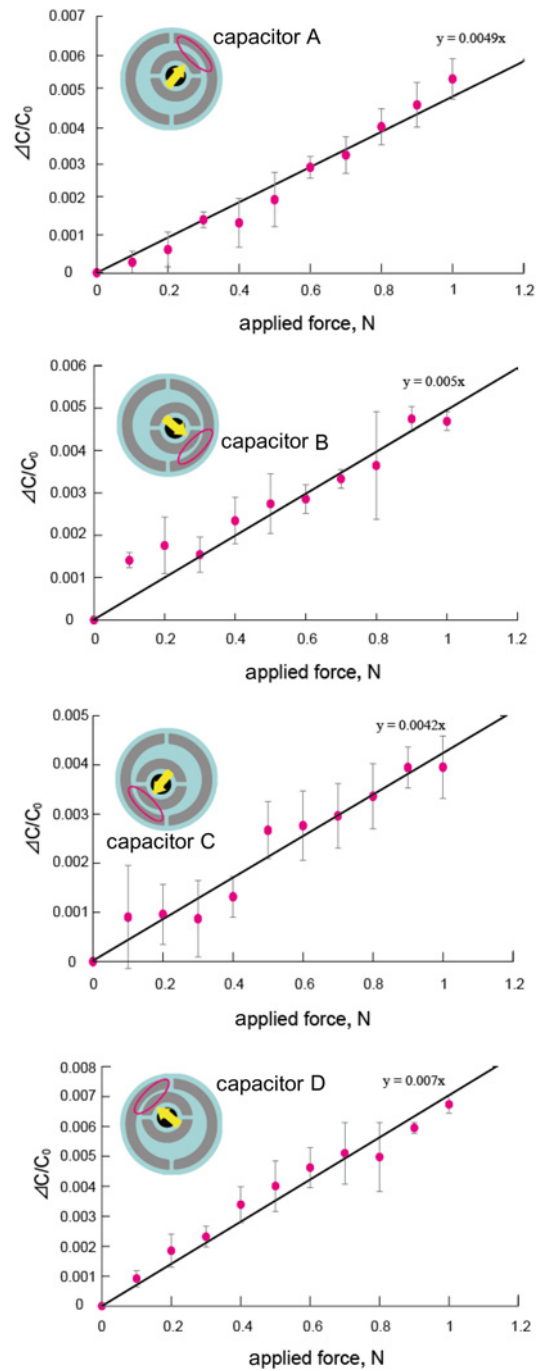


Fig. 7 Relative change in capacitance with force ($n = 5$)

force. C_0 is the initial capacitance. The data points represent average values and standard deviations calculated from five replicate trials. $\Delta C/C_0$ increased with the applied shear force almost linearly, which verified the device concept. The results were fitted using the least-squares method, and the correlation coefficients were found to be 0.9905, 0.9746, 0.9748, and 0.9880 for capacitors A–D, respectively. The sensitivities and initial capacitances C_0 were 0.49, 0.50, 0.42, and 0.7%/N, and 3.87, 4.33, 4.41 and 3.96 pF, for capacitors A–D, respectively. The discrepancies in the sensitivity among the four capacitors originate from manufacturing errors and suggest that calibration is required prior to experiments. As can be seen in Fig. 7, several of the data points contain a large amount of error, which we believe is due to parasitic capacitance and external noise. Insulating the copper wires used and proper grounding would reduce the errors.

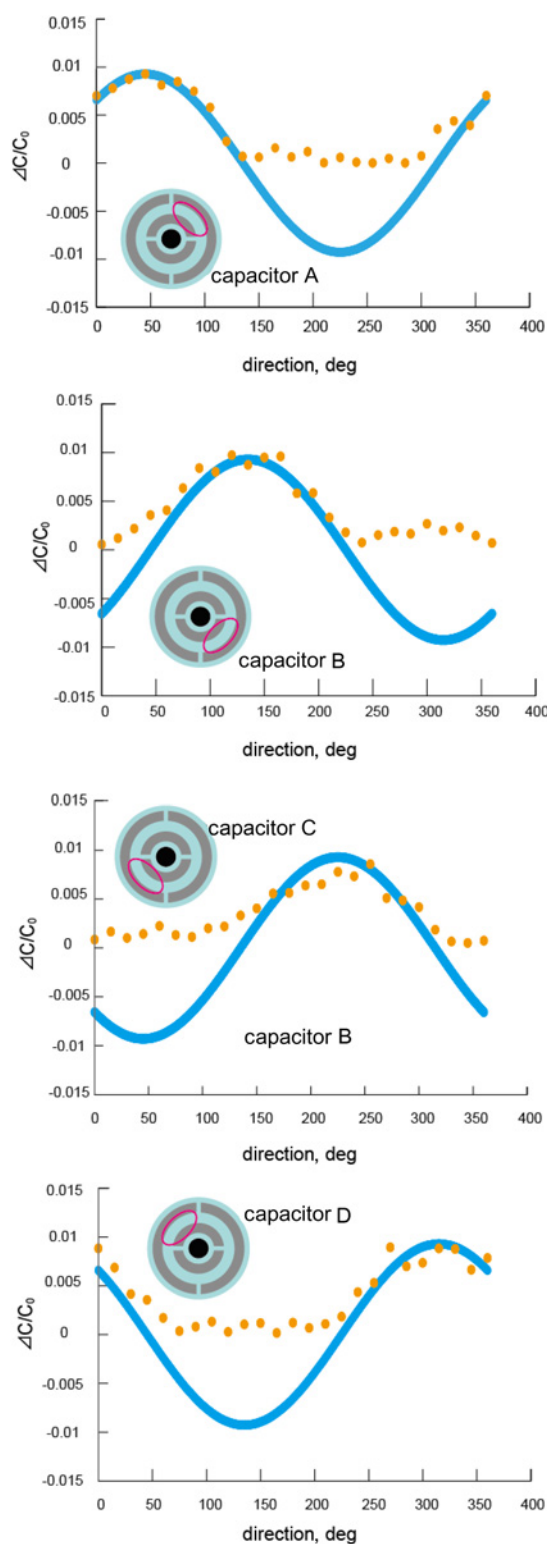


Fig. 8 Relative change in capacitance when force of 1.0 N is applied from different directions

Fig. 8 shows plots of $\Delta C/C_0$ versus θ for capacitors A–D when 1.0 N of force is applied. In this experiment, C_0 was 0.93 pF. The data points represent the measured capacitances for a given angle while the solid line represents the theoretical values derived using (2). When the force is applied to the opposite side of the sensor, the rod came out of the PDMS body and the capacitance does not change. The sensors may suffer from cross-axis coupling due to the flexible PDMS body. Although we did not observe severe

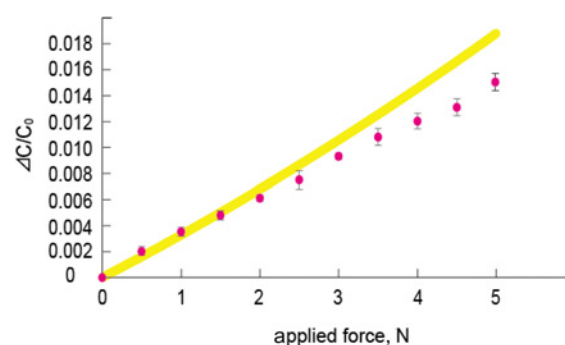


Fig. 9 Relative change in capacitance of bottom sensor with applied force ($n = 5$)

cross talk, we will look further into it in the future. Hysteresis was not observed in the experiments. Based on these results, the top sensor was verified to be able to measure the magnitude and direction of the applied force.

Fig. 9 shows a plot of $\Delta C/C_0$ vs. applied normal force for the bottom sensor. The yellow line represents theoretical values obtained using (4). The data points represent average values and standard deviations calculated from five replicate experiments. Since the palpation force of surgeons was reported to be typically 4.4 N [10], the range of force applied to the bottom sensor was chosen to be 0 to 5.0 N. Both the theoretical and experimental values are almost linear in this range. Equation (4) can be considered to be linear, i.e. the quadratic term can be neglected, when the stress is negligibly small compared to the longitudinal elastic modulus of the polymer. This result indicated a one-to-one correspondence between electrostatic capacitance and force on the bottom sensor and a monotonic increase in electrostatic capacitance with increasing force. The sensitivity of the bottom sensor was found to be 0.3%/N. To measure tissue stiffness, it is essential that the sensor maintain stable vertical contact with the tissue, and this may require an additional mechanism. For example, Peng *et al.* [11] proposed a mechanism whereby a sensor is able to maintain vertical contact with a tissue surface. Further experiments will be conducted to measure the stiffness.

6. Conclusions: 3D microfluidic channels can be used to construct sensor electrodes to form capacitors by encapsulating liquid metal. A miniaturised sensor was demonstrated, which was constructed by assembling eight PDMS layers using liquid PDMS as the glue. By transducing the change in the capacitance to external force, the device can measure both shear and normal forces. The bottom sensor was verified to be able to detect forces ranging from 0 to 5.0 N, which is on the same order of forces typically encountered during endoscopic palpation.

7. Acknowledgment: This work was supported by JST PRESTO (Information and Human), Microsoft Research Asia and JSPS KAKENHI, Grant-in-Aid for Scientific Research (B) 15H03547.

8 References

- [1] Jürgen P., Marion S.: ‘Biophotonics ~visions for better health care~’ (WILEY-VCH Verlag GmbH & Co. KGaA, New Jersey, 2006)
- [2] Robert W.A.: ‘The biology of CANCER’ (Garland Science, Taylor & Francis Group, LLC, New York, 2008)
- [3] Miller B.: ‘Epidemiologic studies in cancer prevention and screening’ (Springer Science + Business Media, New York, 2013)
- [4] Tiwana M.I., Redmond S.J., Lovell N.H.: ‘A review of tactile sensing technologies with applications in biomedical engineering’, *Sens. Actuators*, 2011, **167**, (2), pp. 171–187
- [5] Hu Y., Katragadda R.B., Tu H., *ET AL.*: ‘Bioinspired 3-D tactile sensor for minimally invasive surgery’, 2010, **19**, (6), pp. 1400–1408

- [6] Mckinley S., Garg A., Sen S., *ET AL.*: 'A disposable haptic palpation probe for locating subcutaneous blood vessels in robot-assisted minimally invasive robotic surgery', *Sens. Actuators*, 2004, **2-3**, (115), pp. 447–455
- [7] Nakadegawa T., Miki N.: 'Ballpoint pen like pressure sensor with liquid metal electrodes'. Transducers 2015 Conf., Alaska, 2015
- [8] Hoshi T., Shinoda H.: 'Nonlinear tactile element to sense contact force and area', *Trans. Soc. Instrum. Control Eng.*, 2006, **42**, (7), pp. 727–735
- [9] Wu H., Huang B., Zare R.N.: 'Construction of microfluidic chips using polydimethylsiloxane for adhesive bonding', *Lab Chip*, 2005, **5**, pp. 1393–1398
- [10] Trejos A.L., Jayender J., Perri M.T., *ET AL.*: 'Robot-assisted tactile sensing for minimally invasive tumor localization', *Int. J. Robot. Res.*, 2009, **28**, (9), pp. 1118–1133
- [11] Peng P., Sezen A.S., Rajamani R., *ET AL.*: 'Novel MEMS stiffness sensor for force and elasticity measurements', *Sens. Actuators A*, 2010, **158**, (1), pp. 10–17